Hydrogen - dislocation interactions in a low-copper 7xxx aluminium alloy: About the analysis of interrupted stress corrosion cracking tests

Loïc Oger, Eric Andrieu, Grégory Odemer, Lionel Peguet, Christine Blanc

Hydrogen - dislocation interactions in a low-copper 7xxx aluminium alloy: About the analysis of interrupted stress corrosion cracking tests

L. Oger [a], E. Andrieu [a], G. Odemer [a], L. Peguet [b], C. Blanc [a,*]

[a] CIRIMAT, Université de Toulouse, CNRS, INP-ENSIACET, 4 Allée Emile Monso, BP 44362, 31030, Toulouse Cedex 4, France
[b] Constellium Technology Center, 725 rue Aristide Bergès, CS 10027, 38341, Voreppe cedex, France

Keywords:
A. Fracture behaviour
A. Electron microscopy
B. Aluminium alloys
B. Intermetallics
C. Surface phenomena
D. Plasticity

A B S T R A C T

Aluminium alloys are susceptible to stress corrosion cracking (SCC) in specific conditions, which can be associated with hydrogen embrittlement (HE). Interrupted SCC tests are often performed to evaluate the susceptibility of the samples to a specific environment under mechanical loading. Those tests consist in a pre-corrosion step, which can lead to hydrogen-precharging, followed by a tensile test in air. The present study, performed on a 7046 aluminium alloy, confirmed literature data showing that tensile tests in laboratory air on as-polished samples at sufficiently low strain rates led to a significant hydrogen ingress. Depending on the sample microstructure, various hydrogen - dislocations and dislocations - microstructure interactions could be effective leading to a change in the tensile behaviour of the samples. Such a phenomenon could lead to misinterpret the interrupted SCC tests performed on hydrogen-precharged samples. In the present study, a corrected SCC susceptibility factor was defined to better analyse the interrupted SCC tests.

1. Introduction

The automotive industry is increasingly subjected to standards requiring a major limitation of polluting emissions leading research and development policies to focus on the weight reduction of the vehicle structure by replacing steels with aluminium alloys. In this respect, 7xxx (Al Zn–Mg) aluminium alloys are a promising alternative, due to their high mechanical properties. However, they are also known to be susceptible to stress corrosion cracking (SCC) in some specific conditions. Therefore, a better understanding of the mechanisms involved in SCC conditions would contribute to a metallurgical optimisation of these alloys. Generally, cracks are initiated from defects in relation with forming processes or with localised corrosion (pitting or intergranular corrosion). These local defects can then evolve into cracks according to different types of damage mechanisms such as preferential dissolution of the grain boundaries for alloys susceptible to intergranular corrosion, stress concentration at the crack tip, with mechanisms assisted or not by hydrogen [1–3]. Concerning the 7xxx series aluminium alloys, many studies highlighted the effect of hydrogen during SCC mechanisms [4–8]. Classically, SCC behaviour of aluminium alloys is studied by slow strain rate tests (SSRT) in aqueous environment in order to exacerbate the role of the corrosive environment as well as the adsorption and the diffusivity/transport of the absorbed species [9–11]. The main interest here is that SSRT promote hydrogen-dislocations interactions that constitute a key phenomenon for most of mechanisms proposed to describe SCC behaviour of aluminium alloys. Indeed, previous studies showed that hydrogen diffusion in the lattice or at grain boundaries could be slowed down due to hydrogen trapping on specific microstructural sites. These traps can be classified as reversible (dislocations, vacancies [12], low-angle grain boundaries [13]) or irreversible (precipitates [8,14] and high-angle grain boundaries [15–17]). Concerning the specific case of dislocations, many experimental evidences showed reciprocal interactions between hydrogen and dislocations [18]. A decrease in the elastic interactions between dislocations was observed by transmission electron microscopy (TEM) in a 310S hydrogenated steel, with a decrease in the distance between dislocations [18]. Evidences of a hydrogen effect on dislocation motion in 7075, 7050 and high purity aluminium alloys were also observed [19–21]. Finally, it was also demonstrated that hydrogen could inhibit the cross-slip of dislocations, promoting dislocation piling up [22,23].

Therefore, the manifest interactions between hydrogen and dislocations contribute to explain the macroscopic damage observed after SCC exposure, generally associated with a decrease in the elongation to failure [6,21,24] and characterised by the occurrence of brittle

* Corresponding author.
E-mail address: christine.blanc@ensiacet.fr (C. Blanc).

https://doi.org/10.1016/j.msea.2020.139654

intergranular and transgranular fracture modes (quasi-cleavage) [24, 25]. Among the existing models, the most frequently mentioned are i) the hydrogen-induced dislocation emission (AIDE) model [26] based on hydrogen adsorption in the first atomic layers of the alloy promoting the emission of dislocations at the defect tip, and ii) the hydrogen-enhanced localised plasticity (HELP) model [27] that considers the formation of hydrogen Cottrell atmospheres around dislocations leading finally to enhanced localised plasticity.

For a better understanding of the SCC susceptibility of aluminium alloys, interrupted SCC tests are often performed. They consist in a pre-corrosion step, which can correspond to hydrogen-precharging depending on the electrolyte and on the alloy, followed by a tensile test in air. However, some authors showed that moist air could be associated with embrittlement of aluminium alloys. For example, stress corrosion crack growth rate of two low-copper Al–Zn–Mg–Cu alloys, i.e. AA 7079 and AA 7022 (0.6%–0.9% Cu), and a high-copper alloy, i.e. AA 7075 (1.5% Cu), was investigated by Knight et al. [28] in aqueous chloride and in moist air (AA: aluminium alloy). In moist air, the authors observed crack arrest markings indicating a discontinuous crack growth process, where the crack growth rate between markings could be related to the hydrogen arrival time (by diffusion or transport) up to the process zone, i.e the crack tip plastic zone. The authors highlighted that the rate-determining step was not how fast hydrogen content increased at the grain boundaries by diffusion, but rather the hydrogen embrittlement mechanism occurring at the grain boundaries. More generally, at room temperature, a large body of evidence supports hydrogen environment embrittlement (HEE) as the mechanistic process governing environment-enhanced fatigue crack growth behaviour in aluminium alloys in the presence of water vapor; such embrittlement is observed even at low P_{H2O} values [29–32]. Indeed, Kannan et al. [11] carried out SSRT tests in glycerin and in laboratory air leading to highlight hydrogen absorption from air moisture related to increased degradation. Furthermore, works performed by Holroyd et al. [33] and Mueller et al. [34] focused on the reversibility of HE depending on the strain rate and the testing environment, in particular for SSRT tests performed in laboratory air on hydrogen-precharged samples; the authors demonstrated that laboratory air might counteract the properties recovery, clearly showing that laboratory air was definitively not an inert atmosphere. The influence of the testing environment on tensile tests results was also studied more recently by Dey et al. [35].

In this framework, the present study attempts to provide a better understanding of hydrogen-dislocation interactions and their role on the loss of mechanical properties for a hydrogen-embrittled low-copper aluminium alloy. Tensile tests were carried out in laboratory air under controlled moisture (relative humidity of about 60 %) at various strain rates for an AA 7046 considered at two different metallurgical states, after hydrogen pre-charging in NaCl solution. Reference tests corresponded to tensile tests in the same environment as previously (i.e., laboratory air under controlled moisture) without hydrogen-precharging. However, considering the results obtained by different authors [33–36] relative to SSRT tests performed in laboratory air, the influence of this specific environment during tensile tests, in particular those at low strain rate, was also investigated to help in the interpretation of the results obtained for the hydrogen-precharged samples.

2. Experimental procedure

2.1. Materials and specimen preparation

2.1.1. Material and microstructure characterisation

In the present work, 2-mm thick sheets of a 7046 aluminium alloy (AA 7046) were studied (Constellium Research center, France). The chemical composition of the alloy was Zn (7.4 ± 0.2), Mg (1.5 ± 0.1), Cu (0.16 ± 0.02), Fe (0.20 ± 0.08), other elements (<0.1) and Al (balance) (in wt. %); such a composition corresponded to a low-Cu alloy. The reference metallurgical state, T4, was hot rolled, cold rolled, solution heat treated and then stored at room temperature for two weeks until microstructure stabilisation. The second metallurgical state, named 150/20, was obtained from T4 sheets by applying an artificial ageing treatment at 150 °C for 20 h. The mechanical properties of both metallurgical states are presented in the following; significant differences in their yield strength and ultimate tensile strength are shown. As pointed out by Holroyd in his review paper [37], the comparison of the HE susceptibility of different aluminium alloys is relevant for alloys with similar mechanical resistance. In this paper, the aim was not to conclude about an improvement of the HE susceptibility depending on the heat treatment, but to study the hydrogen-dislocation interactions to help in analysing the results of interrupted tensile tests performed for hydrogen-precharged samples.

Optical microscopy (OM, Olympus PMG3) and scanning electron microscopy (SEM LEO435VP) coupled with energy dispersive X-ray spectroscopy (EDS IMIX analyser) were used to characterise the coarse precipitation. The samples were mechanically ground with SiC paper from grade 1200 to grade 2400, then polished with 9 μm and 3 μm diamond paste, rinsed in distilled water for 30 s in an ultrasonic bath and finally air-dried. Distilled water was used as lubricant during the polishing step. For microstructure characterisation at a finer scale, TEM (JEOL-JEM-2010) was used. The samples were cut as discs of 3 mm in diameter after having been abraded using SiC paper (grade 1200) until a thickness of 100 μm. These discs were finally electropolished in a TenuPol-5 solution (CH_3OH: 900 mL, HNO_3: 300 mL) at -15 °C. The precipitates were also characterised by EDX analyses with a spot size varying from 1.5 to 30 nm and by plotting their electron diffraction patterns.

2.1.2. Tensile specimen preparation

Tensile samples were directly machined in the 2-mm thick sheets by electro-erosion in order to provide samples with a gauge length of 23 mm and a width of 3 mm, as described in a previous paper [24]. The loading direction was the long-transverse (LT) direction of the sheet. Before each tensile test, the samples were mechanically ground with SiC paper (grade 1200) to remove the zone affected by the electro-erosion process. They were then polished with 9 μm and 3 μm diamond paste with distilled water as lubricant, rinsed in distilled water for 30 s in an ultrasonic bath and finally air-dried.

2.2. Hydrogen-precharging and hydrogen content measurements

2.2.1. Hydrogen-precharging

Hydrogen-precharging corresponded to an immersion of the samples at their corrosion potential (E_{corr}) in a 0.6 M NaCl solution. Two types of samples were used, i.e. parallepipedic coupons and tensile samples. For tensile samples, only the gauge length was exposed to the electrolyte, the heads and edges being protected by silicone. The exposed surface area was $15 \times 3\ mm^2$ for the two types of samples, corresponding to the L-LT plane (L, longitudinal and LT, long-transverse). The temperature of both the laboratory and the electrolyte was maintained at 25 °C and samples were tested (for hydrogen amount measurements and tensile tests) less than 5 min after hydrogen-precharging. Samples that were not hydrogen-precharged in NaCl before the tensile tests are referred to as “as-polished” samples.

2.2.2. Hydrogen amount measurements

The global hydrogen amount contained in the samples was measured using a Bruker G8 GALILEO Instrumental Gas Analyser (IGA). The samples were melted in graphite crucibles and the hydrogen amount was quantified by a catharometric method with Argon as vector gaz. For this study, the setup allowed a sensitivity of 0.5 ppm for samples of approximately 300 mg. The near surface of the samples was slightly dry-polished using a 2400 SiC paper before the measurement in order to limit the presence of hydrogen related to the formation of a thin hydrated oxide film during the immersion in NaCl solution [38]. Each

measurement was repeated at least two times.

2.3. Tensile tests

A first set of tensile tests was carried out at strain rates within the range of 10^{-3} to 10^{-6} s^{-1} at room temperature in laboratory air with controlled moisture (relative humidity of about 60 %) on a dual column *MTS* testing machine with a frame capacity of 30 kN. The strain was measured by contact extensometers during the tensile tests. As-polished (i.e., samples without exposure to NaCl) and hydrogen-precharged samples were tested in order to highlight the effects of hydrogen on the mechanical properties and fracture surfaces observed by SEM. Then, a second set of tensile tests was performed on as-polished samples under vacuum, i.e. 1.10^{-5} mbar, in order to evaluate the effect of hydrogen from moist air on the tensile curves. For those tests under vacuum, a *MTS* testing machine with a frame capacity of 5 kN was used and tests were carried out in an environmental test chamber. The sample strain was measured by means of a laser extensometer. It is of major importance here to note that additional tensile tests in laboratory air were performed for as-polished samples using this experimental setup, i.e. the MTS testing machine with the 5 kN frame capacity, in order to allow a relevant comparison between tensile tests in air and under vacuum for as-polished samples. The only difference was the techniques used to measure the sample strain, i.e. by means of a laser extensometer for under-vacuum tests, as said above, and by contact extensometers for tests in air. As mentioned later in the results section, this did not interfere with the robustness of the conclusions drawn from the results.

3. Results and discussion

3.1. Hydrogen-precharging in NaCl solution

Prior to the tensile tests, coupons (L-LT surfaces) of both T4 and 150/20 samples of AA 7046 were immersed in a 0.6 M NaCl solution at their corrosion potential. Those preliminary immersion tests were performed for durations between 1 and 72 h. Due to the high chloride content of the electrolyte, they led to the growth of corrosion defects. The aim here was to take advantage of the susceptibility to localised corrosion of AA 7046 in order to introduce hydrogen in both T4 and 150/20 samples. Indeed, it is well known that localised corrosion mechanisms imply a local acidification step inside the corrosion defects associated with an exacerbated proton reduction, and finally with the adsorption and diffusion of hydrogen into the metal lattice [1–8]. After the immersion tests, global hydrogen amount was measured in order to establish a relationship between the global hydrogen amount inserted into the samples and the immersion duration time in NaCl.

After 1 h of exposure, only matrix dissolution (not shown) was observed for both T4 and 150/20 samples around coarse precipitates, i.e. Al_3Fe and Al_3Ti, that are nobler than the matrix and act as cathodic sites [8]. After 72 h of exposure, pitting corrosion occurred for T4 state (Fig. 1a), whereas only matrix dissolution was observed for 150/20 sample (Fig. 1b). This difference in corrosion behaviour was explained by the presence for 150/20 samples of intragranular $MgZn_2$ precipitates (Fig. 2b), that were not present in the T4 samples (Fig. 2a). Indeed, several works showed that the presence of magnesium and zinc in solid solution contributed to reduce the corrosion potential of the matrix [39–42]. Moreover, it is also known that zinc in solid solution decreases the breakdown resistance of the Al_2O_3 passive layer. Consequently, the precipitation of intragranular $MgZn_2$ precipitates during the heat treatment at 150 °C led to an increase in the corrosion potential of the matrix, so that the gap between the corrosion potential of coarse precipitates and that of the matrix was reduced. This led to a lower susceptibility of 150/20 samples to pitting corrosion, than for T4 samples. Finally, OM observations of cross-sections (Fig. 1c) also showed that no intergranular corrosion occurred for both T4 and 150/20 samples of AA 7046. This result was consistent with the low copper content of this alloy, which led to a relatively low potential gap between the matrix and the precipitate free zone (PFZ) surrounding the grain boundaries. Moreover, it was of interest to note that the pits were not deeper than a few micrometers.

Fig. 3 shows, for both samples, an increase in the hydrogen content with exposure time to NaCl, confirming that hydrogen uptake occurs due to the corrosion processes. It could be noticed also that the hydrogen amount increased in the first exposure times for both samples, but seemed to stabilise for longer durations, which was in good agreement with pitting corrosion kinetics. Indeed, experimental results obtained by Blanc et al. suggested that the pit propagation followed a time-dependent relationship described by a $t^{1/3}$ law [43]. However, whatever the immersion time in NaCl, the hydrogen content of 150/20 sample was significantly lower than for T4 sample. This result was consistent with the lower corrosion susceptibility previously observed for the 150/20 sample. It was also in agreement with our previous work about the influence of trapping on the hydrogen diffusion in low-copper 7xxx aluminium alloy [8]. Indeed, SKPFM investigations had demonstrated that the hardening incoherent precipitates formed during the ageing treatment at 150 °C acted as hydrogen trapping sites and thus limited the hydrogen diffusion in the alloy. In order to compare the behaviour of both 150/20 and T4 samples during tensile tests in air, it was necessary to introduce the same hydrogen amount inside the samples; therefore, on the basis of the results (Fig. 3), it was decided to immerse T4 and 150/20 samples in 0.6 M NaCl during 1 h and 72 h, respectively, before the tensile tests. With such a pre-corrosion duration time, it was possible to have similar hydrogen contents for both samples, i.e. 9 wppm (Fig. 3). Moreover, because both T4 and 150/20 samples were only susceptible to matrix dissolution or pitting corrosion with shallow pits, and not to intergranular corrosion, it was assumed that the mechanical behaviour of the hydrogen-precharged samples during the tensile tests was mainly affected by hydrogen, and not by the surface corrosion defects.

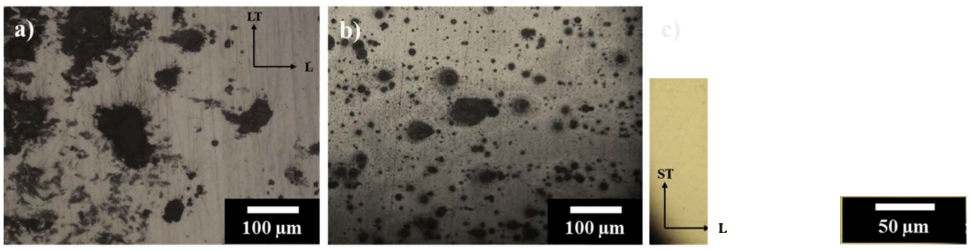

Fig. 1. Optical micrographs of AA 7046 at both T4 (a, surface and c, cross-section) and 150/20 (b) metallurgical states after 72 h in 0.6 M NaCl. (Color online only; two-columns). (For interpretation of the references to colour in this figure legend, the reader is referred to the Web version of this article.)

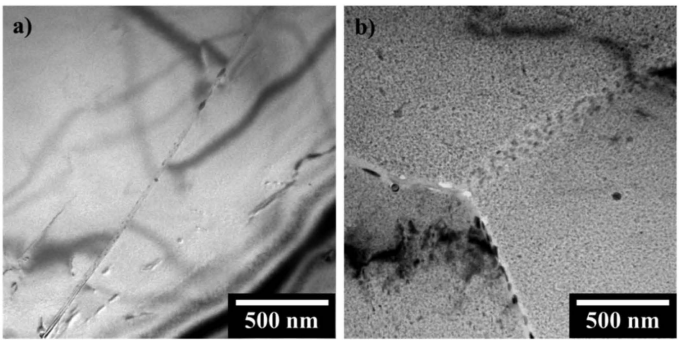

Fig. 2. TEM images of a) T4 and b) 150/20 samples of AA 7046. (Color online only; two-columns).

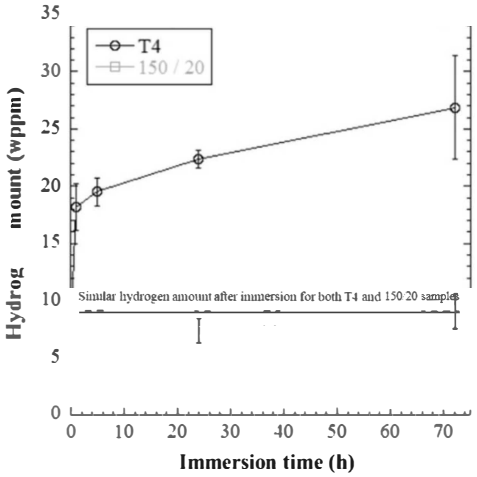

Fig. 3. Hydrogen content versus immersion time in 0.6 M NaCl solution for T4 and 150/20 samples. (Black and white figure; single column).

3.2. *First observations of the hydrogen-dislocation interactions*

Fig. 4a and b shows a comparison of the tensile behaviour in laboratory air under controlled moisture (relative humidity of about 60 %) of T4 and 150/20 samples, respectively, at an intermediate strain rate (10^{-3} s^{-1}) and a slow strain rate (10^{-6} s^{-1}) for as-polished (i.e., without hydrogen-precharging) and hydrogen-precharged (9 wppm of hydrogen) samples. It is reminded here that all the tensile curves were plotted using the same test frame for a relevant comparison of the results. At first, it must be noticed that, for as-polished samples, tensile curves plotted at 10^{-3} s^{-1} logically showed an increase in the yield strength (from 365 MPa for T4 to 435 MPa for 150/20) in parallel to a decrease in the elongation to failure (from 18 % for T4 to 13.5 % for 150/20) for 150/20 sample as compared to T4 sample. This behaviour was consistent with the literature [44,45], and was attributed to the overageing of the 150/20 sample. In their work, Albrecht et al. [21] studied different metallurgical states for an AA 7075 and gave the same conclusions. In particular, the formation of intragranular hardening precipitates, i.e. η' and η-$MgZn_2$, limited the dislocation motion, which explained the higher yield stress for 150/20 sample, as compared to the T4 sample. Moreover, the dislocations pile-ups around these precipitates led to a premature failure and thus to a lower elongation to failure for the 150/20 sample as compared to the T4 sample. Surprisingly, the work hardening ($d\sigma/d\varepsilon$) was stronger for the T4 sample than for the 150/20 sample. This could be explained by solute atom-dislocations interactions and the formation of dislocation forests (dislocations threading the glide plane) leading to a strong increase in the hardness of the grains [45]. In the 150/20 sample, the dislocations interacted preferentially with the hardening intragranular precipitates, thus limiting the interactions between dislocations. Moreover, comparison of the curves obtained at 10^{-3} s^{-1} and 10^{-6} s^{-1}, for two given samples, e.g. two as-polished T4 samples, showed that there was no significant change in the constitutive mechanical laws related to the strain rate, considering a cumulated plastic strain lower than 2 %; the major change was a decrease in the elongation to failure that could be attributed either to a purely mechanical effect (strain rate sensitivity and strain localisation) or to an influence of hydrogen from moist air. Indeed, for given samples, the exposure time to moist air was longer during a 10^{-6} s^{-1} test than during a 10^{-3} s^{-1} test.

Therefore, attention was then paid to the comparison between results obtained for as-polished samples for one part, and for hydrogen-precharged samples for the other part. Tensile tests under vacuum will be presented in the following to go further in the understanding and strengthen the conclusions drawn from the results given hereafter. Focusing now on the hydrogen-dislocation interactions, it was relevant to think that all the mechanisms described above, and involving dislocations, could be affected by the presence of hydrogen. This was demonstrated by the present results; indeed, Fig. 4 also showed that, at a strain rate of 10^{-3} s^{-1}, for both T4 and 150/20 samples, the elongation to failure was decreased for hydrogen-precharged samples as compared to as-polished samples. However, for both T4 and 150/20 samples, the constitutive mechanical laws of the microstructures were not modified by hydrogen and surface corrosion defects. The same observations were done for tensile tests performed at 10^{-6} s^{-1}. Therefore, it could be concluded that hydrogen had no effect on crack initiation step on the surface of smooth tensile specimen, but it affected the final fracture, in agreement with another study about Ni-base alloy [46]. Furthermore, another interesting result was the decrease in the elongation to failure for as-polished T4 and 150-20 specimens when the strain rate decreased from 10^{-3} to 10^{-6} s^{-1}, as previously mentioned. Two hypotheses could be proposed to explain this result: either the decrease in the elongation to failure could be explained by a change in the fracture mechanisms with modification of the strain rate and related to a modification in dislocations motion mechanisms, or it could be due to the fact that the laboratory air was not an inert environment, especially for slow strain rate, as clearly demonstrated in the literature [5,11,47,48]. Indeed, at slow strain rate, by analogy to fatigue behaviour of 2xxx aluminium alloys [29–32], hydrogen adsorption from air humidity could occur on the metal surface, followed by hydrogen absorption and transport by

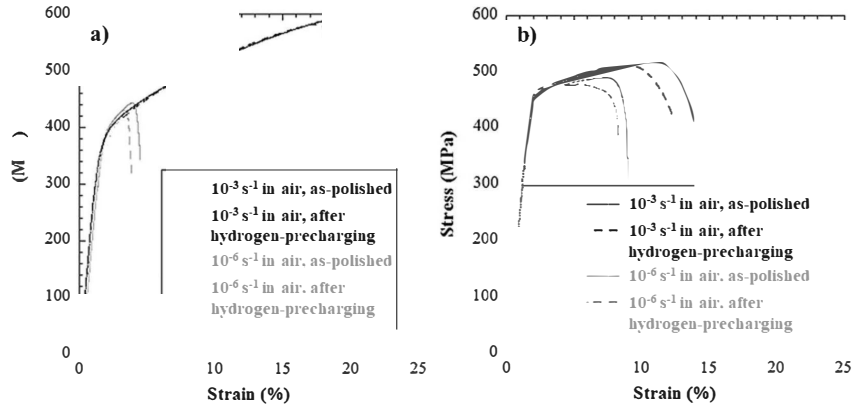

Fig. 4. Tensile curves obtained for a) T4 and b) 150/20 samples. Experiments were performed in laboratory air under controlled moisture, for two strain rates, i.e. 10^{-3} and 10^{-6} s^{-1}, for both as-polished (i.e., without hydrogen-precharging) and hydrogen-precharged samples (i.e., after 1 h and 72 h in 0.6 M NaCl for T4 and 150/20 samples, respectively). All tensile tests were performed using the same test frame (frame capacity of 30 kN). (Black and white figure; two-columns).

dislocations leading to a premature failure due to a modification of fracture modes. As noted in the introduction, several works studied the effect of the moisture content on the ductility loss during SCC tests performed in laboratory environment for high strength aluminium alloys [2,11,36,49]. They highlighted the major role of moisture present in the laboratory atmosphere, and showed that the ductility ratio decreased with an increase in relative humidity. For example, the SCC behaviour of an underaged AA 7010 was tested in glycerin and the results were compared with those obtained in 3.5% NaCl solution and in laboratory air [11]. Results clearly showed that laboratory atmosphere could not be considered as an inert atmosphere as the alloy underwent SCC failure due to hydrogen embrittlement related to the relative humidity of the test environment, which had been also clearly demonstrated by various authors for a wide range of 7xxx series alloys [21,33,36,50]. As an example, Scamans et al. [2] reported that, in the laboratory air, the crack growth rate of Al–6Zn–3Mg alloy was controlled by a continuous interaction between the specimen and the water vapor.

3.3. *Evaluation of the influence of moist air on the tensile behaviour of T4 and 150/20 samples*

Previous results showed that no modification of the constitutive mechanical laws due to the sole effect of the strain rate was observed for cumulated plastic strains lower than 2 % within the range of strain rate studied [10^{-6} s^{-1} –10^{-3} s^{-1}] (Fig. 4). This suggested strongly that changes in the mechanical behaviour of the samples, with a decrease in the elongation to failure during tensile tests in laboratory air, in particular for slow strain rates, were related to hydrogen ingress. Therefore, at first, in order to analyse more precisely the influence of the strain rate applied during tensile tests in laboratory air on the elongation to failure of the samples, i.e. on the hydrogen-dislocations interactions, complementary tensile tests in laboratory air were carried out at 10^{-4} and 10^{-5} s^{-1} (tensile curves not shown) for as-polished samples. A strain rate susceptibility factor, referred to as I_{srsf}, was defined (Eq. (1)):

$$I_{srsf}(10^{-x}) = \frac{E_{f\ as-polished\ sample}(10^{-x}) - E_{f\ as-polished\ sample}(10^{-3})}{E_{f\ as\ polished\ sample}(10^{-3})} \qquad \text{Eq. 1}$$

where E_f (10^{-x}) (respectively 10^{-3}) was the elongation to failure measured for a tensile test performed at 10^{-x} s^{-1} (respectively 10^{-3} s^{-1}). The I_{srsf} values were assumed to quantify the influence of the strain rate on the deleterious effect of hydrogen on mechanical properties. However, the influence of the strain rate on the constitutive equations and deformation modes, independently of hydrogen effect, as shown by Holroyd et al. [37], could not be neglected in a first time, even though, as said above, previous results suggested that, for AA 7046, within the range of strain rate studied, the approximation was relevant. This will be checked in the following with tensile tests performed under vacuum. Fig. 5 shows the I_{srsf} factor versus the strain rate for both as-polished T4 and 150/20 samples. The results showed a significant increase in the I_{srsf} values when the strain rate decreased, as soon as the strain rate was lower than 10^{-4} s^{-1}, for both T4 and 150/20 samples. The results also showed a more significant influence of the strain rate on the decrease in elongation to failure for the T4 sample, as compared to the 150/20 sample. Those results suggested that the decrease in elongation to failure for both as-polished T4 and 150/20 samples, when the strain rate applied during the tensile tests in laboratory air decreased, was essentially due to HE; they suggested the existence of a critical strain rate, i.e. 10^{-4} s^{-1}, for these experimental conditions, for which hydrogen-dislocation interactions were efficient. Those results were in

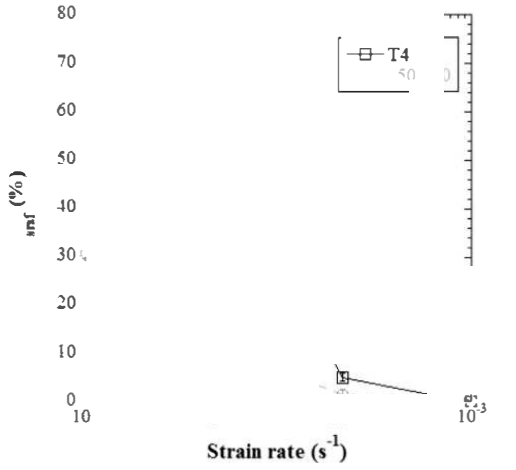

Fig. 5. Strain rate susceptibility factor (I_{srsf}) versus the strain rate for both T4 and 150/20 samples. Tensile tests performed in laboratory air for as-polished samples. (Black and white figure; single column).

agreement with the data provided by Holroyd and Scamans who showed that, at sufficiently low strain rates, alloys in susceptible tempers showed a loss of ductility in laboratory air (relative humidity of about 55–60 %, similar to that of the present work), as compared to vacuum [48]. They showed that the loss of ductility resulted from intergranular crack initiation and growth [48]. The difference in HE susceptibility between T4 and 150/20 samples could be explained by referring to the hardening precipitation in 150/20 sample that reduced the hydrogen diffusion into the material, as showed by the previous hydrogen content measurements (Fig. 3). Indeed, the trapping effect of hardening precipitates could decrease the apparent hydrogen diffusion coefficient, as shown in other studies [8,24]. Those precipitates could also reduce the dislocations mobility and thus the hydrogen transport by dislocations-related phenomena.

Fig. 6 shows the fracture surfaces for both T4 (Fig. 6a) and 150/20 (Fig. 6e) samples, after tensile tests in laboratory air at 10^{-6} s^{-1} for as-polished samples. For all fracture surfaces, two areas could be distinguished: a ductile zone in the core of the specimen (Fig. 6b and f, bottom) and a brittle zone close to the sample surface exposed to laboratory air (Fig. 6c, d and 6f, top). For a description in detail, for T4 samples, a ductile intergranular fracture was observed in the core of the specimens (Fig. 6b), whereas brittle intergranular fracture close to the surface specimen (Fig. 6c) and transgranular fracture (quasi-cleavage) at the interface between brittle intergranular and ductile intergranular areas (Fig. 6d) were observed. For 150/20 samples, from the surface down to the core of the specimens, brittle intergranular, brittle transgranular (quasi-cleavage) and ductile transgranular fractures with dimples were observed (Fig. 6f). As shown in our previous studies [8,24], the ductile intergranular fracture mode for T4 sample and ductile transgranular fracture mode for 150-20 sample were the usual fracture modes observed for those samples in the absence of hydrogen or for a low amount of hydrogen, i.e. in the core of the specimen in this case. It was worth noting here that such a behaviour was unusual for 7xxx series alloys; Albrecht et al. showed, for AA 7075, ductile transgranular fracture for solution heat-treated samples and ductile intergranular for aged samples due to strain localisation in the PFZ [21]. In the present case, for AA 7046, in the absence of hydrogen or for a low amount of hydrogen, strain localisation at the grain boundaries was mainly observed for the T4 sample. Considering the results provided by Holroyd et al. who showed that, for commercial 7xxx series alloys, intergranular cracking

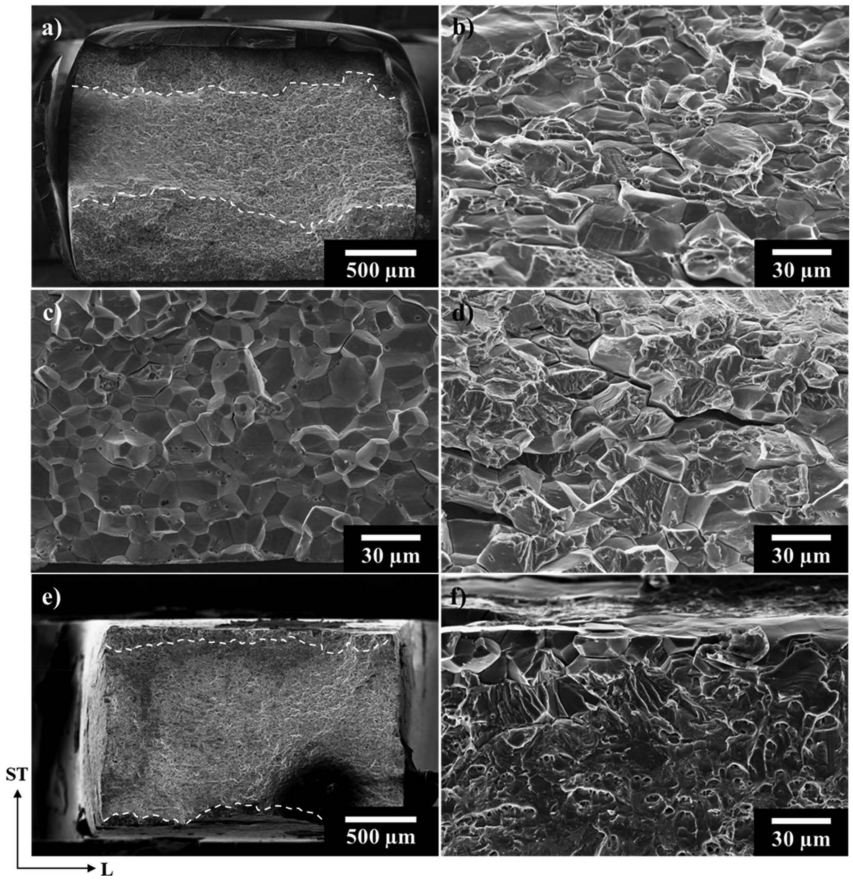

Fig. 6. SEM micrographs of the fracture surfaces of the as-polished AA 7046 after tensile tests at 10^{-6} s^{-1} for the T4 (a,b,c,d) and 150/20 (e,f) samples. External areas delimited by the white batched lines correspond to brittle fracture mode. Micrograph b) shows the usual ductile intergranular fracture in the core of the T4 specimens. Micrographs c) and d) show brittle intergranular fracture mode close to the surface specimen, and brittle transgranular fracture mode at the interface between brittle intergranular and ductile areas, respectively for the T4 sample. Micrograph f) shows, from the surface down to the core for the 150/20 sample, brittle intergranular, brittle transgranular (quasi-cleavage) and ductile transgranular fracture modes. (Color online only; two-columns).

could be only observed when an alloy had been previously pre-exposed to an environment known to promote an enhanced susceptibility to intergranular cracking [36,48], it was suspected that the ductile intergranular fracture mode observed for T4 sample in the core of the specimen had to be related to the presence of a low amount of hydrogen. The brittle intergranular and brittle transgranular (quasi-cleavage) fracture areas observed for both T4 and 150/20 samples close to the surface exposed to laboratory air confirmed the crucial role of hydrogen resulting from moisture in relation with a slow strain rate, i.e. slow dislocation motion, on the fracture surfaces. According to Albrecht et al. [21], two conditions are required to lead to brittle intergranular fracture in a 7xxx aluminium alloy with equiaxed grains, i.e. sufficient normal stress applied on the grain boundaries and a high enough hydrogen concentration at the grain boundaries in order to lower the intergranular cohesion stress. This suggested that, in the present study, dislocations had transported hydrogen from moist air up to the grain boundaries. Furthermore, three additional observations deserved to be pointed out:

- At first, it was noticed that the brittle fracture zones for tensile tests performed in laboratory air at 10^{-6} s^{-1} for as-polished samples were observed all along the sample surface exposed to air (Fig. 6a and e). This suggested that tensile tests performed in laboratory air at 10^{-6} s^{-1} led to a homogenous hydrogen absorption at the sample surface. On the contrary, only localised brittle fracture zones were observed for hydrogen-precharged samples tested at 10^{-3} s^{-1}, as shown in previous studies [8,24]. This could be easily explained by considering a very heterogeneous hydrogen distribution when hydrogen-precharging resulted from an immersion in NaCl: indeed, in this case, hydrogen was produced due to the localised corrosion processes, i.e. matrix dissolution around coarse precipitates or pits [8,24]. Therefore, the differences in hydrogen distribution between samples hydrogen-precharged in NaCl, and as-polished samples when mechanically tested at 10^{-6} s^{-1}, could, at least partially, explain that the decrease in elongation to failure between the as-polished and the hydrogen-precharged samples for tensile tests at 10^{-3} s^{-1} was lower than the decrease observed between tensile tests performed in laboratory air on as-polished samples at 10^{-3} and 10^{-6} s^{-1}.
- Then, for the 150/20 sample, the depth of the brittle zones was shallower (~10–20 μm, Fig. 6e) than for the T4 sample (~100–200 μm) (Fig. 6a), probably due, as previously discussed, to the presence of intragranular hardening precipitates for 150/20 sample that led to a decrease in the apparent hydrogen diffusion coefficient and also reduced the dislocation mobility and thus hydrogen transport by dislocations [24].

Therefore, fracture surfaces analyses confirmed the hypothesis of hydrogen absorption during tensile tests performed in laboratory air at 10^{-6} s^{-1}. In order to provide another experimental proof of hydrogen ingress, hydrogen contents were measured by melting method after tensile tests in laboratory air at 10^{-3}, 10^{-4}, 10^{-5} and 10^{-6} s^{-1} for as-polished samples: the tests were interrupted after 1 % of strain in the plastic domain for hydrogen content measurements. The results, summarised in Fig. 7a, showed that a decrease in the strain rate led to an increase in the global hydrogen amount measured in the samples, from 7 ± 1 wppm at 10^{-3} s^{-1} to 17 ± 1 wppm at 10^{-6} s^{-1} for the T4 sample, and from 8 ± 1 wppm at 10^{-3} s^{-1} to 16 ± 3 wppm at 10^{-6} s^{-1} for the 150/20 sample. It was interesting to note that the hydrogen amount absorbed by an as-polished sample during an interrupted tensile test in laboratory air at 10^{-6} s^{-1} was larger than the hydrogen content measured after a pre-immersion step in NaCl (1 h and 72 h for T4 and 150/20 samples, respectively), i.e. 9 wppm; this was in agreement with previous comments about the fracture surfaces (Fig. 6). Furthermore, it was of interest to note that a similar hydrogen content was absorbed for both as-polished T4 and 150/20 samples after interrupted tensile tests in laboratory air at 10^{-6} s^{-1}, whereas previous observations of the fracture surfaces showed that the 150/20 sample was less embrittled than the T4 sample considering the extent of the brittle fracture areas (Fig. 6). This confirmed, in agreement with our previous work [8], that the hydrogen trapped near hardening η' and η-$MgZn_2$ precipitates in the 150/20 samples was less detrimental that the hydrogen in the lattice and at the grain boundaries, considering that, for T4 sample, there was only diffusible hydrogen and hydrogen trapped at the grain boundaries.

To go further in the description of the hydrogen - dislocations interactions, the decrease in elongation to failure evaluated through I_{srsf} was analysed as a function of the evolution of the global hydrogen amount in the sample (Fig. 7b). It must be reminded here that the global hydrogen amount was measured after 1% of plastic deformation for both T4 and 150/20 samples, which might lead to underestimated values as compared to the hydrogen amounts introduced inside the samples just before the failure. However, a comparative analysis was relevant. Fig. 7b showed that I_{srsf} values varied with the square root of the global hydrogen amount, in agreement with literature [51,52]. In particular, Wang et al. [51] studied the influence of the hydrogen during SSRT on notched AISI 4135 steel samples. A square root relationship was highlighted from experimental results between the hydrogen segregation at

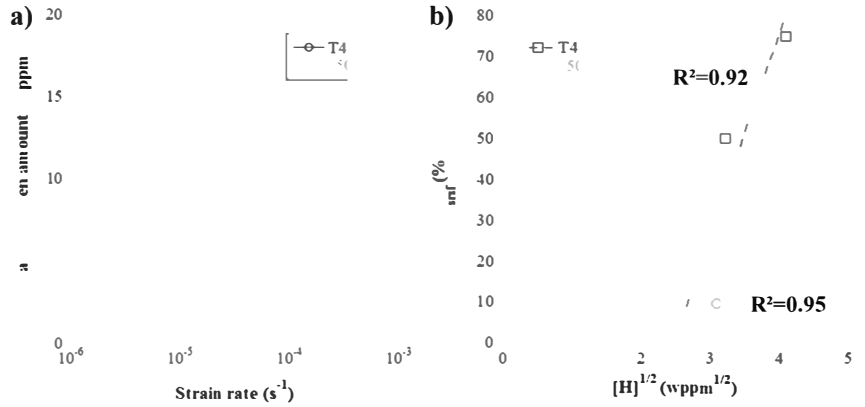

Fig. 7. a) Global hydrogen amount versus the strain rate during the tensile tests performed in laboratory air on as-polished samples of AA 7046 (T4 and 150/20 samples). The hydrogen amount was measured after 1% of plastic deformation. b) Evolution of the strain rate susceptibility factor (I_{srsf}) with the square root of the hydrogen concentration measured after 1% of plastic deformation for both T4 and 150/20 samples. (Black and white figure; two-columns).

grain boundaries and their cohesive strength at a local scale. This type of relationship was supported by other works [53,54].

Finally, to strengthen the demonstration of the influence of moist air on the tensile behaviour of AA 7046 samples at slow strain rates, complementary tensile tests were carried out under vacuum (10^{-5} mbar) for two strain rates, i.e. 10^{-3} s^{-1} and 10^{-6} s^{-1}, on as-polished T4 (Fig. 8a) and 150/20 (Fig. 8b) samples. In order to allow a relevant comparison with tensile tests performed in laboratory air, a new set of tensile tests were performed in laboratory air for as-polished samples using the same loading frame as for tests under vacuum. One could note that there was no significant difference between the tensile curves plotted in laboratory air using the 30 kN loading frame (Fig. 4) and those plotted with the 5 kN loading frame (Fig. 8). All these experiments aimed in particular to investigate the influence of the sole strain rate on the mechanical response of both metallurgical states. The results showed that, under vacuum, for both T4 and 150/20 samples, the mechanical responses, i.e. the flow rules, were independent of the strain rate. Furthermore, for both samples, the tensile curves plotted at 10^{-3} s^{-1} in laboratory air were similar to those obtained under vacuum. The slight difference in elongation to failure between the tensile curves at 10^{-3} s^{-1} in laboratory air and tensile curves at 10^{-3} s^{-1} under vacuum was due to the difference in precision between the two techniques used to measure the sample strain, i.e. by means of a laser extensometer for under-vacuum tests and by contact extensometers for tests in laboratory air (as indicated in the experimental part). On the contrary, for both samples, significant differences were observed between the tensile curves plotted at 10^{-6} s^{-1} in air and under vacuum. Therefore, the results confirmed the role of hydrogen issued from moist air on the decrease in the elongation to failure previously observed for tensile tests performed at 10^{-6} s^{-1} in laboratory air.

Moreover, the fracture surfaces led to the same conclusions: indeed, brittle fracture areas disappeared under vacuum, for both T4 and 150/20 samples (Fig. 9). Moreover, for the T4 sample, the ductile intergranular fracture mode observed in laboratory air in the sample core was replaced by a ductile transgranular fracture mode with wide dimples. This result might suggest that, even for tests performed at 10^{-3} s^{-1} in moist air, hydrogen was absorbed inside the T4 samples in agreement with previous hydrogen content measurements (Fig. 7), and leading to a change in the fracture mode, from ductile transgranular to ductile intergranular. However, the ductile intergranular fracture mode might also be due to the presence of residual hydrogen trapped at the grain boundaries at the end of the elaboration and shaping processes. If this last hypothesis was the good one, therefore the results would suggest a desorption of residual hydrogen during under-vacuum tensile tests. Whatever the hypothesis, the observation of only ductile transgranular fracture mode for T4 sample for tensile tests under vacuum was in agreement with Holroyd et al. results [36,48]. For a better explanation, hydrogen content measurements were performed for T4 and 150/20 as-polished samples before and after a desorption treatment under vacuum with a duration time equal to the tensile test duration. The results showed a slight decrease in the hydrogen content from 7 ± 1 to 5 ± 0.5 wpppm for T4 sample during the desorption treatment, whereas no desorption was measured for 150/20 samples. For T4 samples, even if the hydrogen loss was relatively low, the repeatability obtained for 5 measurements suggested that the decrease could be considered as reliable. Therefore, the disappearance of the ductile intergranular fracture mode during under-vacuum tensile tests for T4 samples might be due to the desorption of residual hydrogen trapped at grain boundaries. Furthermore, with such a conclusion, it could be assumed also that the amount of residual hydrogen in T4 samples could also contribute to explain the slight differences in tensile curves between tensile tests performed at 10^{-3} s^{-1} in laboratory air and those at 10^{-3} s^{-1}/10^{-6} s^{-1} under vacuum. Finally, hydrogen trapping by strengthening precipitates in 150/20 samples could explain that no hydrogen desorption was observed for these samples. This result was in good agreement with literature that generally proposed for aluminium alloys a lower hydrogen trapping binding energy for grain boundaries than for hardening precipitates [12].

Considering all the results previously described, a mechanism could be proposed to explain the influence of the environment during tensile tests performed in laboratory air at low strain rate, i.e. 10^{-6} s^{-1}, for both T4 and 150/20 AA 7046 samples. According to Eq. (2), hydrogen uptake should be related with the formation of the native oxide layer or with the hydration of the surface [2,19].

$$2Al^{3+} + 3H_2O \rightarrow Al_2O_3\ (hydrated) + 6H^+ \quad (2)$$

The properties of the oxide layer formed on the sample surface in different environments were discussed by Dey et al. [35]. The authors showed that the adherence and consistency of the film depended on the environment, so that the oxide film could prevent or not from hydrogen embrittlement; the interaction between the oxide film and hydrogen depended also on the strain rate. Then, the presence of hydrogen in the first atomic layer under the alloy surface should lead to a lattice distortion promoting the nucleation of dislocations during the tensile tests. Hydrogen atoms could form Cottrell atmospheres around dislocations and could be transported during tensile tests at slow strain rates

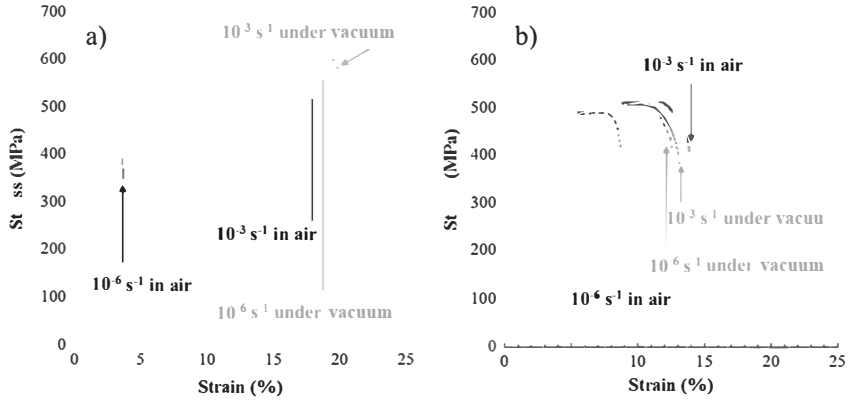

Fig. 8. Tensile curves plotted at 10^{-3} and 10^{-6} s^{-1} under vacuum for as-polished a) T4 and b) 150/20 samples. For a relevant comparison, new tensile tests in laboratory air under controlled moisture were performed for as-polished samples using the same loading frame (frame capacity of 5 kN) as for tensile tests under vacuum. (Black and white figure; two-columns).

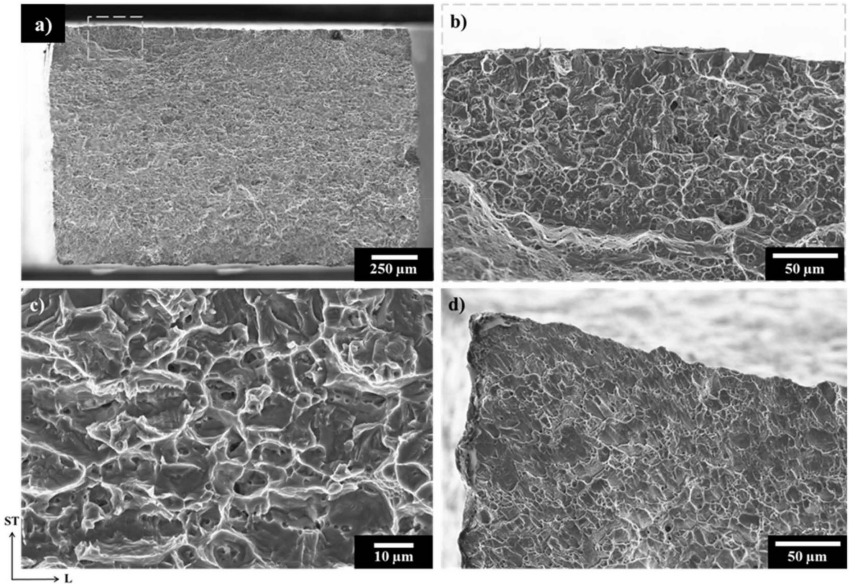

Fig. 9. SEM micrographs of the fracture surfaces after tensile tests at 10^{-6} s^{-1} under vacuum: a) global fracture surface for the as-polished T4 sample. Focus on b) and c) ductile fracture areas for the as-polished T4 sample, and d) ductile fracture areas for the as-polished 150/20 sample. (Color online only; two-columns).

deeper inside the bulk. This could lead to changes in the fracture modes. Indeed, in the case of T4 sample with a low hydrogen amount (e.g for tensile tests performed at a high strain rate), the deformation was localised around grain boundaries, leading to ductile intergranular fracture mode [8,24]. But, with a slow strain rate, hydrogen could be dragged by dislocations from the surface down to the core of the samples, and it could segregate at the grain boundaries leading to both a decrease in the intergranular cohesion strength [4,55], and an accumulation of dislocations at the grain boundaries due to a decrease in the dislocation-dislocation interactions [18]. This would lead to a brittle intergranular fracture mode at the sample surface, where the hydrogen amount was high. Far from the surface, the hydrogen amount at the grain boundaries would not be high enough to induce brittle intergranular fracture mode, but the stress concentration at the crack tip would lead to a quasi-cleavage fracture mode. Concerning the 150/20 samples, during the tensile tests in laboratory air at 10^{-6} s^{-1}, the slow dislocations motion and the continuous production of hydrogen at the alloy surface would promote also the hydrogen penetration, leading to hydrogen amounts higher than those measured after an immersion in NaCl. However, for the 150/20 sample, the deformation would be mainly localised around hardening precipitates, with precipitates - dislocations interactions that slowed down the dislocation motion. Hydrogen would be mostly trapped at the hardening precipitates and would affect the grain boundaries only at the extreme surface. This would lead to a hydrogen - affected fracture zone less deep than for the T4 sample.

3.4. About the analysis of the results from tensile tests performed in laboratory air on hydrogen-precharged samples

Previous results showed that it was necessary to consider the influence of the environment to analyse the tensile tests results obtained for hydrogen-precharged samples, the tensile behaviour of those samples being likely to be influenced by both the hydrogen from moist air and the hydrogen from the precharging step (corrosion-induced hydrogen). However, going back to the mechanism proposed above, it is true that a change in the oxide layer present on the sample surface after exposure to the NaCl electrolyte, as compared to as-polished samples, should be considered. It might be assumed that the modified oxide layer present on hydrogen-precharged samples would not let the hydrogen from moist air absorb as easy as for as-polished samples. At the present time, no experimental data could be given to assess this hypothesis. However, as mentioned previously, data from the literature showed that the structure of hydrated oxide films was affected by relative humidity and by alloy composition [35,56,57]. Moreover, it was reported that the ordering of adsorbed water changed with relative humidity [48,58,59], and it could be assumed that the composition of the hydrated oxide would have some influence on this phenomenon. For example, on aluminium oxide at relative humidity below 10%, water adsorbs to the surface forming a hydroxide layer. In the intermediate range between 10 and 70% relative humidity, water adsorbs molecularly in a 3–12 Å range thick structured over-layer [60]. At high relative humidity, above 70%, a more disordered layer forms, which is consistent with a liquid-like layer [56]. Therefore, even though hydrogen from moist air influenced the tensile tests results performed on hydrogen-precharged samples, in agreement with literature data [33–36], it was difficult to claim that it was exactly the same influence as for as-polished samples. Nevertheless, it was previously showed that the hydrogen from moist air was more damaging than hydrogen introduced from pre-corrosion step (with the pre-corrosion conditions used). Furthermore, it could be also argued that during the tensile tests, the progressive increase in the stress applied should lead to a local breakdown of the modified hydrated oxide layer, limiting its barrier effect and thus giving hydrogen from moist air a direct access to the surface. As a consequence, the influence of hydrogen from moist air on the tensile behaviour of the hydrogen-precharged samples could not be neglected. Therefore, in order to allow the sole

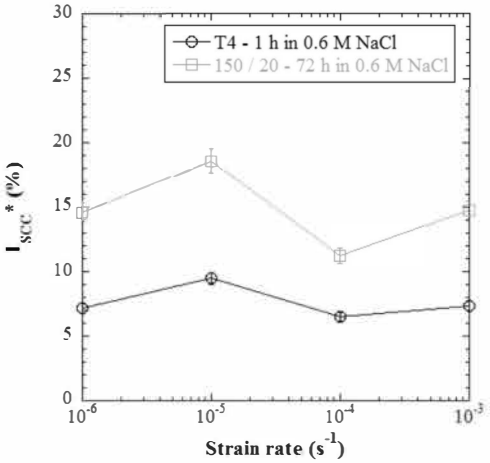

Fig. 10. Corrected stress corrosion cracking factor (I_{SCC}*) versus the strain rate for both T4 and 150/20 samples. Tensile tests were performed under laboratory air after hydrogen-precharging corresponding to an exposure to 0.6 M NaCl during 1 h and 72 h for T4 and 150/20 samples, respectively. (Black and white figure; two-columns).

influence of hydrogen-precharging on the tensile behaviour of the samples to be evaluated, it was necessary to differentiate the influence of hydrogen from moist air and that of hydrogen introduced during the precharging step. In that framework, a new corrected stress corrosion cracking factor (I_{SCC}*) was defined as follows, for hydrogen-precharged samples:

$$I_{SCC}{}^{*}(10^{-x}) = \frac{E_{f\ as-polished\ sample\ tested\ in\ air}(10^{-x}) - E_{f\ hydrogen-precharged\ sample\ tested\ in\ air}(10^{-x})}{E_{f\ as-polished\ sample\ tested\ under\ vacuum}(10^{-x})} \quad (3)$$

With this definition, I_{SCC*} values reflected the influence on the tensile results of hydrogen from the precharging step only. Such an approach could be related to that previously developed by Holroyd and Hardie, who addressed the same issue using a 'reduction in area' fracture parameter [33]. Fig. 10 shows I_{SCC*} values as a function of the strain rate for both hydrogen-precharged T4 and 150/20 samples. At first, results clearly showed that I_{SCC*} values were significantly lower than I_{srsf} values, which confirmed, for these precharging conditions, the major influence of hydrogen from moist air. Then, it could be observed that I_{SCC*} values were lower for T4 samples than for 150/20 samples, whatever the strain rate, and contrary to I_{srsf} values. Finally, it could be noticed that no significant influence of the strain rate on the I_{SCC*} values could be highlighted for both T4 and 150/20 samples. For the 150/20 sample, such a result could be explained once more by considering that the corrosion-induced hydrogen was trapped by hardening precipitates, and therefore it was not likely to interact with dislocations. Such a result had already been observed in a previous study: it had been shown that the hydrogen diffusion depth was unchanged after three weeks of desorption [8], suggesting the irreversible nature of the trapping sites at ambient temperature, even though hydrogen uptake might reverse after extended recovery times. However, concerning the T4 samples, the same study showed that the major part of the hydrogen introduced in the alloy was diffusible hydrogen [8]. As a consequence, hydrogen might be dragged by dislocations, which was not highlighted in the present study at slow strain rates. Such a result might be explained by considering that the dislocations were already saturated by hydrogen from moist air, so that no interaction between the dislocations and corrosion-induced hydrogen was possible. This was in agreement with previous observations and conclusions showing that, for these precharging conditions, the tensile behaviour of hydrogen-precharged samples was mainly influenced by hydrogen from moist air. However, those explanations had to be balanced taking into account that the pre-exposure conditions could influence the crack growth rate and the depth of hydrogen embrittlement [61]. Therefore, to sum up, all the results described in the present study clearly showed that the analysis of SCC results had to be conducted carefully: for interrupted SCC tests, to evaluate the residual mechanical properties of the pre-corroded samples, i.e. hydrogen-precharged samples, by performing tensile tests in laboratory air, the influence of moist air had to be taken into account, in agreement with literature data previously cited.

4. Conclusion

This study focused on the interactions between the hydrogen and the dislocations during tensile tests at slow strain rates in the AA 7046 in order to help in the analysis of interrupted SCC tests.

1. At first, results confirmed literature data showing that laboratory air could not be considered as an inert environment during tensile tests when a sufficiently low strain rate was applied. Global hydrogen amount measurements showed an increase in the hydrogen absorbed into the alloy during tensile tests in laboratory air when the strain rate decreased from 10^{-3} s^{-1} to 10^{-6} s^{-1}. This was attributed to hydrogen absorption from air moisture followed by hydrogen transport by dislocations.
2. The influence of moist air on the tensile behaviour of AA 7046 samples depended on the sample microstructure. The mechanism proposed suggested that, for T4 sample, the hydrogen was dragged by dislocations, forming Cottrell atmospheres, up to the grain boundaries. The high local hydrogen concentrations reached at the grain boundaries would contribute to a decrease in the local cohesion strength and to a more localised deformation, leading to brittle intergranular fracture mode. For the 150/20 sample, for a same hydrogen amount, a lower impact of hydrogen from moist air on the tensile behaviour was observed. This was explained by hardening precipitates that limited the dislocation motion and also acted as strong hydrogen trapping sites. As a consequence, it was estimated that a lower amount of hydrogen reached the grain boundaries, explaining the less extended brittle intergranular fracture areas observed on the fracture surfaces for 150/20 samples.
3. When interrupted SCC tests were performed, i.e. tensile tests in laboratory air on hydrogen-precharged samples, the influence of hydrogen from moist air could not be neglected. The coupling effect between the hydrogen formed due to the hydration of the oxide film in contact with moist air and active deformation could lead to erroneous conclusions concerning the influence of hydrogen introduced during the pre-corrosion step. In the present study, only a low influence of the hydrogen introduced during the precharging step on the tensile behaviour of hydrogen-precharged samples was observed due to a strong influence of hydrogen from moist air that was

assumed to saturate the dislocations considered as trapping sites for hydrogen.

Data availability

The raw/processed data required to reproduce these findings cannot be shared at this time as the data also forms part of an ongoing study.

Declaration of competing interest

The authors declare that they have no known competing financial interests or personal relationships that could have appeared to influence the work reported in this paper.

CRediT authorship contribution statement

L. Oger: Investigation, Formal analysis, Validation, Visualization, Methodology, Data curation, Writing - original draft, Writing - review & editing. **E. Andrieu:** Methodology, Writing - review & editing. **G. Odemer:** Methodology, Supervision, Writing - original draft, Writing - review & editing. **L. Peguet:** Funding acquisition, Resources, Project administration, Writing - review & editing. **C. Blanc:** Funding acquisition, Methodology, Project administration, Supervision, Validation, Conceptualization, Data curation, Writing - original draft, Writing - review & editing.

Acknowledgement

The authors thank the ANRT for their financial support (Loïc Oger's PhD thesis). They also thank Constellium (Centre de Recherche de Voreppe, France) for their financial support.

References

[1] W. Gruhl, Stress corrosion cracking of high strength aluminum alloys, Z. Metallkd. 75 (1984) 819–826, https://doi.org/10.1002/chin.198507377.
[2] G.M. Scamans, R. Alani, P.R. Swann, Pre-exposure embrittlement and stress corrosion failure in Al-Zn-Mg alloys, Corrosion Sci. 16 (7) (1976) 443–459, https://doi.org/10.1016/0010-938X(76)90065-2.
[3] K. Hebert, Trapping of hydrogen absorbed in aluminum during corrosion, Electrochim. Acta 168 (2015) 199–205, https://doi.org/10.1016/j.electacta.2015.03.198.
[4] L. Christodoulou, H. Flower, Hydrogen embrittlement and trapping in Al6%-Zn-3%-Mg, Acta Metall. 28 (4) (1980) 481–487, https://doi.org/10.1016/0001-6160(80)90138-8.
[5] N.J.H. Holroyd, G.M. Scamans, Stress corrosion cracking in Al-Zn-Mg-Cu aluminum alloys in saline environments, Metall. Mater. Trans. A 44 (3) (2012) 1230–1253, https://doi.org/10.1007/s11661-012-1528-3.
[6] D. Najjar, T. Magnin, T.J. Warner, Influence of critical surface defects and localized competition between anodic dissolution and hydrogen effects during stress corrosion cracking of a 7050 aluminium alloy, Mater. Sci. Eng. 238 (2) (1997) 293–302, https://doi.org/10.1016/S0921-5093(97)00369-9.
[7] M.O. Speidel, Stress corrosion cracking of aluminum alloys, Metall. Trans. A. 6 (4) (1975) 631–651, https://doi.org/10.1007/BF02672284.
[8] L. Oger, M.C. Lafouresse, G. Odemer, L. Peguet, C. Blanc, Hydrogen diffusion and trapping in a low copper 7xxx aluminium alloy investigated by Scanning Kelvin Probe Force Microscopy, Mater. Sci. Eng. 706 (2017) 126–135, https://doi.org/10.1016/j.msea.2017.08.119.
[9] C. Meng, D. Zhang, L. Zhuang, J. Zhang, Correlations between stress corrosion cracking, grain boundary precipitates and Zn content of Al-Mg-Zn alloys, J. Alloys Compd. 655 (2016) 178–187, https://doi.org/10.1016/j.jallcom.2015.09.159.
[10] T. Magnin, A. Chambreuil, B. Bayle, The corrosion-enhanced plasticity model for stress corrosion cracking in ductile fcc alloys, Acta Mater. 44 (4) (1996) 1457–1470, https://doi.org/10.1016/1359-6454(95)00301-0.
[11] M.B. Kannan, V.S. Raja, A.K. Mukhopadhyay, Determination of true stress corrosion cracking susceptibility index of a high strength Al alloy using glycerin as the non-corrosive atmosphere, Scripta Mater. 51 (11) (2004) 1075–1079, https://doi.org/10.1016/j.scriptamat.2004.08.002.
[12] H. Kamoutsi, G.N. Haidemenopoulos, V. Bontozoglou, P.V. Petroyiannis, SpG. Pantelakis, Effect of prior deformation and heat treatment on the corrosion-induced hydrogen trapping in aluminium alloy 2024, Corrosion Sci. 80 (2014) 139–142, https://doi.org/10.1016/j.corsci.2013.11.021.
[13] G.A. Young, J.R. Scully, The diffusion and trapping of hydrogen in high purity aluminum, Acta Metall. 46 (18) (1998) 6337–6349, https://doi.org/10.1016/S1359-6454(98)00333-4.
[14] M.O. Speidel, in: A.R. Troiano, R. Gibala, R.F. Hehemann (Eds.), Hydrogen Embrittlement and Stress Corrosion Cracking of Aluminium Alloys in: Hydrogen Embrittlement and Stress Corrosion Cracking, American Society for Metals, 1984, pp. 271–296.
[15] J.K. Park, A.J. Ardell, Precipitation at grain boundaries in the commercial alloy Al 7075, Acta Metall. 34 (12) (1986) 2399–2409, https://doi.org/10.1016/0001-6160(86)90143-4.
[16] N. Ben Ali, D. Tanguy, R. Estevez, Effects of microstructure on hydrogen-induced cracking in aluminum alloys, Scripta Mater. 65 (3) (2011) 210–213, https://doi.org/10.1016/j.scriptamat.2011.04.008.
[17] G.M. Pressouyre, A classification of hydrogen traps in steel, Metall. Trans. A. 10 (1979) 1571–1573, https://doi.org/10.1007/BF02812023.
[18] I.M. Robertson, The effect of hydrogen on dislocation dynamics, Eng. Fract. Mech. 68 (6) (2001) 671–692, https://doi.org/10.1016/S0013-7944(01)00011-X.
[19] G.M. Bond, I.M. Robertson, H.K. Birnbaum, The influence of hydrogen on deformation and fracture processes in high-strength aluminum alloys, Acta Metall. 35 (9) (1987) 2289–2296, https://doi.org/10.1016/0001-6160(87)90076-9.
[20] G.M. Bond, I.M. Robertson, H.K. Birnbaum, Effects of hydrogen on deformation and fracture processes in high-purity aluminium, Acta Metall. 36 (8) (1988) 2193–2197, https://doi.org/10.1016/0001-6160(88)90320-3.
[21] J. Albrecht, I.M. Bernstein, A.W. Thompson, Evidence for dislocation transport of hydrogen in aluminum, Met. Trans., A 13A (1982) 811–820, https://doi.org/10.1007/BF02642394.
[22] P.J. Ferreira, I.M. Robertson, H.K. Birnbaum, Hydrogen effects on the interaction between dislocations, Acta Mater. 46 (5) (1998) 1749–1757, https://doi.org/10.1016/S1359-6454(97)00349-2.
[23] P.N. Anyalebechi, Hydrogen diffusion in Al-Li alloys, Metall. Trans. B 21 (4) (1990) 649–655, https://doi.org/10.1007/BF02654243.
[24] L. Oger, B. Malard, G. Odemer, L. Peguet, C. Blanc, Influence of dislocations on hydrogen diffusion and trapping in an Al-Zn-Mg aluminium alloy, Mater. Des. 180 (2019) 107901, https://doi.org/10.1016/j.matdes.2019.107901.
[25] A.S. El-Amoush, An investigation of hydrogen-induced hardening in 7075-T6 aluminum alloy, J. Alloys Compd. 465 (1–2) (2008) 497–501, https://doi.org/10.1016/j.jallcom.2007.10.126.
[26] S.P. Lynch, Comments on "A unified model of environment-assisted cracking", Scripta Mater. 61 (3) (2009) 331–334, https://doi.org/10.1016/j.scriptamat.2009.02.031.
[27] C.D. Beachem, A new model for hydrogen-assisted cracking (hydrogen "embrittlement"), Metall. Trans., B 3 (2) (1972) 441–455, https://doi.org/10.1007/BF02642048.
[28] S.P. Knight, K. Pohl, N.J.H. Holroyd, N. Birbilis, P.A. Rometsch, B.C. Muddle, R. Goswami, S.P. Lynch, Some effects of alloy composition on stress corrosion cracking in Al-Zn-Mg-Cu alloys, Corrosion Sci. 98 (2015) 50–62, https://doi.org/10.1016/j.corsci.2015.05.016.
[29] J. Petit, G. Henaff, C. Sarrazin-Baudoux, I. Milne, R.O. Ritchie, B. Karihaloo, Environmentally assisted fatigue in the gaseous atmosphere, in: Comprehensive Structural Integrity, Chapter: 6.05 - Environmentally Assisted Fatigue in the Gaseous Atmosphere, Pergamon, 2003, pp. 211–280, https://doi.org/10.1016/B0-08-043749-4/06130-9.
[30] R.P. Wei, M. Gao, Hydrogen embrittlement and environmentally assisted crack growth, in: N.R. Moody, A.W. Thompson (Eds.), Hydrogen Effects on Materials Behavior, 1990, pp. 789–816. The minerals, metals & materials Society, Warrendale.
[31] R.P. Gangloff, Environment sensitive fatigue crack tip processes and propagation in aerospace aluminum alloys, in: Fatigue 2002, Materials Advisory Services, 2002, pp. 3401–3433. West Midlands, UK.
[32] J.T. Burns, Effect of Water Vapor Pressure on the Fatigue Crack Propagation of Aerospace Aluminum Alloys 7075-T651 and 2199-T86 in: Proceedings of NACE DoD Corrosion Conference, NACE International, 2013.
[33] N.J.H. Holroyd, D. Hardie, The role of hydrogen in the environment-sensitive fracture of aluminium alloys, in: 3rd International Congress on Hydrogen and Materials, 1982, pp. 659–663. Paris, France.
[34] M. Mueller, I.M. Bernstein, A.W. Thompson, Recovery Behavior of hydrogen charged 7075-T6 aluminum, Scripta Metall. 17 (1983) 1039–1042, https://doi.org/10.1016/0036-9748(83)90447-7.
[35] S. Dey, I. Chattoraj, Interaction of strain rate and hydrogen input on the embrittlement of 7075 T6 aluminum alloy, Mater. Sci. Eng. 661 (2016) 168–178, https://doi.org/10.1016/j.msea.2016.03.010.
[36] N.J.H. Holroyd, D. Hardie, Strain-rate effects in the environmentally assisted fracture of a commercial high-strength aluminum alloy 7049, Corrosion Sci. 21 (2) (1981) 129–144, https://doi.org/10.1016/0010-938X(81)90097-4.
[37] N.J.H. Holroyd, Environment-induced cracking of high-strength aluminum alloys, in: Environment-induced Cracking of Metals Proceedings, Nace, 1989, pp. 311–345.
[38] C.E. Buckley, H.K. Birnbaum, Characterization of the charging techniques used to introduce hydrogen in aluminum, J. Alloys Compd. 330 (2002) 649–653, https://doi.org/10.1016/S0925-8388(01)01496-7.
[39] J.C. Lin, H.L. Liao, W.D. Jehng, C.H. Chang, S.L. Lee, Effect of heat treatments on the tensile strength and SCC-resistance of AA7050 in an alkaline saline solution, Corrosion Sci. 48 (10) (2006) 3139–3156, https://doi.org/10.1016/j.corsci.2005.11.009.
[40] A. Cassell, G.E. Thompson, X. Zhou, A. Afseth, H. Dunlop, M.-A. Kulas, L. Peguet, G. Scamans, Microstructure and corrosion behaviour of low copper 7xxx aluminium alloy, Surf. Interface Anal. 45 (10) (2013) 1604–1609, https://doi.org/10.1002/sia.5226.

[41] P.K. Rout, M.M. Ghosh, K.S. Ghosh, Microstructural, mechanical and electrochemical behaviour of a 7017 Al-Zn-Mg alloy of different tempers, Mater. Char. 104 (2015) 49–60, https://doi.org/10.1016/j.matchar.2015.03.025.
[42] N. Birbilis, R.G. Buchheit, Electrochemical characteristics of intermetallic phases in aluminum alloys, J. Electrochem. Soc. 152 (4) (2005) B140–B151, https://doi.org/10.1149/1.1869984.
[43] C. Blanc, G. Mankowski, Pit propagation rate on the 2024 and 6056 aluminium alloys, Corrosion Sci. 40 (2–3) (1998) 411–429, https://doi.org/10.1016/S0010-938X(97)00147-9.
[44] P.K. Rout, M.M. Ghosh, K.S. Ghosh, Microstructural, mechanical and electrochemical behaviour of a 7017 Al-Zn-Mg alloy of different tempers, Mater. Char. 104 (2015) 49–60, https://doi.org/10.1016/j.matchar.2015.03.025.
[45] J.C.F. Millett, N.K. Bourne, M.R. Edwards, The effect of heat treatment on the shock induced mechanical properties of the aluminium alloy, 7017, Scripta Mater. 51 (10) (2004) 967–971, https://doi.org/10.1016/j.scriptamat.2004.07.020.
[46] F. Galliano, E. Andrieu, J.-M. Cloue, G. Odemer, C. Blanc, Effect of temperature on hydrogen embrittlement susceptibility of alloy 718 in Light Water Reactor environment, Int. J. Hydrogen Energy 42 (33) (2017) 21371–21378, https://doi.org/10.1016/j.ijhydene.2017.06.211.
[47] H. Yamada, M. Tsurudome, N. Miura, K. Horikawa, N. Ogasawara, Ductility loss of 7075 aluminum alloys affected by interaction of hydrogen, fatigue deformation, and strain rate, Mater. Sci. Eng. 64 (2015) 194–203, https://doi.org/10.1016/j.msea.2015.06.084.
[48] N.J.H. Holroyd, G.M. Scamans, Crack propagation during sustained-load cracking of Al-Zn-Mg-Cu aluminum alloys exposed to moist air or distilled water, Metall. Mater. Trans. 42 (2011) 3979–3998, https://doi.org/10.1007/s11661-011-0793-x.
[49] D. Hardie, N.J.H. Holroyd, R.N. Parkins, Reduced ductility of high-strength aluminum alloy during or after exposure to water, Met. Sci. J. 13 (11) (1979) 603–610, https://doi.org/10.1179/msc.1979.13.11.603.
[50] S.P. Lynch, Mechanisms of environmentally assisted cracking in Al-Zn-Mg single crystals, Corrosion Sci. 22 (1982) 925–937, https://doi.org/10.1016/0010-938X(82)90062-2.
[51] M. Wang, E. Akiyama, K. Tsuzaki, Effect of hydrogen and stress concentration on the notch tensile strength of AISI 4135 steel, Mater. Sci. Eng. 398 (2005) 37–46, https://doi.org/10.1016/j.msea.2005.03.008.
[52] G.W. Wille, J.W. Davis, Hydrogen in Titanium Alloys, U.S. Department of Energy, McDonnell Douglas Astronautics Company-St. Louis Division, 1981. Contract No DE-AC02-77ET 52039.
[53] J. Kameda, C.J. Mcmahon, Solute segregation and hydrogen-induced intergranular fracture in an alloy steel, Metall. Trans. 14A (1983) 903–911, https://doi.org/10.1007/BF02644295.
[54] S. V Nair, J.K. Tien, A plastic flow induced fracture theory for KI_{SCC}, Metall. Trans. A. 16 (12) (1985) 2333–2340, https://doi.org/10.1007/BF02670433.
[55] N. Ben Ali, R. Estevez, D. Tanguy, Heterogeneity of grain boundaries in 5xxx and 7xxx aluminum alloys and its influence on intergranular toughness, Eng. Fract. Mech. 97 (2012) 1–11, https://doi.org/10.1016/j.engfracmech.2012.10.015.
[56] H.A. Al-Abadleh, V.H. Grassian, FT-IR study of water adsorption on aluminum oxide surfaces, Langmuir 19 (2) (2002) 341–347, https://doi.org/10.1021/la026208a.
[57] P.R. Underhill, A.N. Rider, Hydrated oxide film growth on aluminium alloys immersed in warm water, Surf. Coating. Technol. 192 (2–3) (2005) 199–207, https://doi.org/10.1016/j.surfcoat.2004.10.011.
[58] B. Cheng, B. Tian, C. Xie, Y. Xiao, S. Lei, Highly sensitive humidity sensor based on amorphous Al_2O_3 nanotubes, J. Mater. Chem. 21 (6) (2011) 1907–1912, https://doi.org/10.1039/C0JM02753G.
[59] Z.S. Feng, X.J. Chen, J.J. Chen, J. Hu, A novel humidity sensor based on alumina nanowire films, J. Phys., D 45 (22) (2012) 1–6, https://doi.org/10.1088/0022-3727/45/22/225305.
[60] X. Deng, T. Herranz, C. Weis, H. Bluhm, M. Salmeron, Adsorption of water Cu_2O and Al_2O_3 thin films, J. Phys. Chem. C 112 (26) (2008) 9668–9672, https://doi.org/10.1021/jp800944r.
[61] R. Hermann, N.J.H. Holroyd, Environment sensitive fracture of AA 7475 using shadow optical method of caustics, Mater. Sci. Technol. 2 (1986) 1238–1244, https://doi.org/10.1179/026708386790328344.